SAR image sidelobe suppression network based on SVA

Dezhi Liu, Yuxi Suo, Fun For

ABSTRACT

In Synthetic Aperture Radar (SAR) imaging, sidelobe effects can obscure weak targets, thereby impacting the accuracy of target detection and recognition. Traditional Spatially Variant Apodization (SVA) methods, while effective for range sidelobe suppression, exhibit significant limitations in azimuth processing and are highly dependent on the Nyquist sampling rate. To address these challenges, this paper proposes SVA-Net, a deep learning-based sidelobe suppression network that integrates the weighted filtering mechanism of SVA with the feature learning capabilities of Convolutional Neural Networks (CNN). This integration enhances azimuthal sidelobe suppression performance and reduces sensitivity to sampling rates. Furthermore, a discriminator is introduced to recover mainlobe energy. Experimental results on small-sized SAR datasets demonstrate that SVA-Net achieves effective sidelobe suppression, offering an efficient and intelligent solution for high-precision SAR image processing. The proposed method not only overcomes the limitations of traditional approaches but also significantly improves the fidelity of SAR images within the tested data size constraints, paving the way for advanced applications in SAR imagery analysis.

Key words: SAR images, Sidelobe suppression, Spatially Variant Apodization (SVA), Deep learning

1. INTRODUCTION

Synthetic Aperture Radar [1](SAR) is extensively utilized in applications such as ground target monitoring, marine exploration, and military reconnaissance [2]. SAR imaging technology holds unique advantages, particularly under complex weather conditions, due to its capability to penetrate cloud layers and effectively image at night. This makes it an indispensable component of remote sensing technology. In SAR systems, Linear Frequency Modulated (LFM) signals are the most commonly used transmission pulses, providing excellent range resolution.

However, the pulse response of SAR images typically exhibits a Sinc function shape along both the azimuth and range directions [3]. The main lobe represents the primary reflection area of the signal, while sidelobes refer to regions outside the main lobe. In SAR imaging, the amplitude difference between the main lobe and peak sidelobes is generally 13.26 dB, and the dynamic range of SAR images can reach up to 50 dB [4]. This implies that weak scattering targets, such as small vessels or low-reflectivity ground objects, may be obscured by the sidelobe signals surrounding strong scattering targets like large buildings or aircraft, resulting in significant noise and interference. This sidelobe effect is particularly severe when targets are close to clutter, impacting detection and recognition, especially for targets with complex or faint features.

Furthermore, for certain complex structures such as ships and aircraft, their scattering characteristics in SAR images can be distorted due to the sidelobe effect, affecting structural identification. The resultant degradation in image quality not only reduces the accuracy of target detection but also interferes with subsequent tasks such as target classification, tracking, and analysis. Therefore, sidelobe suppression is a critical task in SAR image processing.

Existing methods for sidelobe suppression can be broadly categorized into three types: filter-based approaches [4,5], modification of transmitted pulses [6], and spectrum deformation techniques [7]. Filter-based methods suppress two-dimensional sidelobes by applying specially designed filters in either the frequency domain or spatial domain. Depending on whether the filter parameters adapt to the processing location, these filters can be classified as static or spatially variant filters. Static filters involve frequency-domain windowing, which can effectively suppress sidelobes but broaden the main lobe, thereby reducing image resolution. Dynamic filters, primarily based on Spatially Variant Apodization (SVA) [4], process the original complex image using different weighting functions. Due to the varying impulse responses of different weighting functions, the results differ accordingly. The minimum value among these processed results is then selected to achieve the effect of sidelobe suppression.

SVA sidelobe suppression methods exhibit significant limitations when handling complex scenes, particularly their sensitivity to sampling rate changes and poor azimuthal suppression. With the widespread application of deep learning in signal processing, CNN have demonstrated strong feature extraction and pattern recognition capabilities, offering new solutions to these challenges. Therefore, this paper proposes a novel sidelobe suppression network, SVA-Net, which integrates the filtering mechanism of SVA algorithms with the adaptive feature learning ability of deep learning, creating

an end-to-end SAR image sidelobe suppression model. This method overcomes the limitations imposed by sampling rates on traditional algorithms and significantly improves azimuthal sidelobe suppression, providing innovative high-precision processing solutions for SAR images. Furthermore, a discriminator is introduced to recover mainlobe energy.

This paper is organized as follows: Section 2 details the basic principles of SVA algorithms and the shortcomings of existing sidelobe suppression methods; Section 3 describes the architecture and implementation details of SVA-Net, including the design of the weight generation module and the filter generation module; Section 4 presents experimental settings and result analyses, validating the suppression effectiveness of the network across different SAR images; finally, Section 5 summarizes the research findings and outlines future improvement directions.

2. SVA-Net

2.1 Spatial Variability Adjustment

Figure 1 illustrates the SAR image before and after applying the SVA algorithm. It clearly shows significant sidelobe suppression in the range direction, though there remains considerable room for improvement in the azimuth direction.

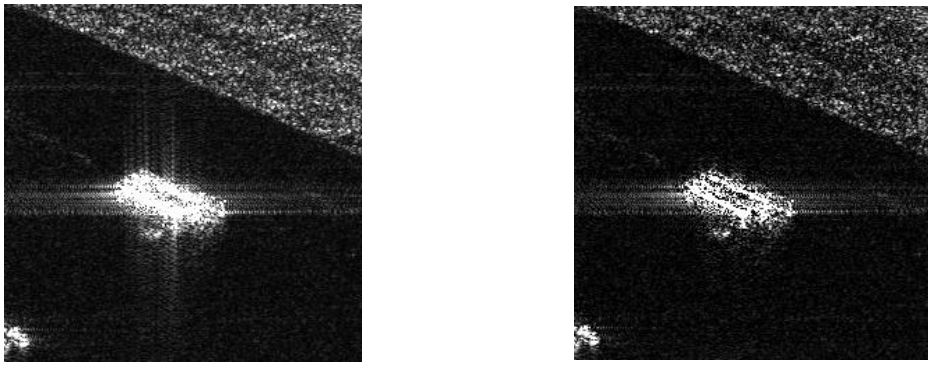

(a) Original Image (b) Image After SVA Processing

Figure 1. SVA Algorithm.

The design of the SVA algorithm is based on the Nyquist sampling rate condition. When the sampling rate deviates from this condition in practical applications, its sidelobe suppression performance significantly deteriorates. In SAR image processing, the sampling interval in the range direction is typically small, and the signal is more likely to satisfy or closely approach the Nyquist sampling rate. As a result, the SVA algorithm exhibits relatively stable sidelobe suppression performance in the range direction, effectively highlighting weak targets.

In contrast, the azimuth resolution is influenced by the length of the antenna's synthetic aperture and the platform's motion trajectory. The motion errors and variations in the sampling rate can lead to under-sampling or over-sampling, resulting in a significant reduction in the SVA algorithm's suppression performance in the azimuth direction. This issue is particularly prominent in complex scenarios with non-uniform sampling or motion errors.

Based on the above analysis, this paper proposes the following improvements:

- Eliminate the SVA algorithm's strict dependence on the Nyquist sampling rate to enhance its robustness under different sampling conditions.
- Improve the sidelobe suppression performance in the azimuth direction to overcome the performance bottlenecks in existing methods.

2.2 Construction of SVA-Net

The sidelobe interference characteristics of SAR images in the range and azimuth directions are similar. However, due to the sensitivity of the SVA algorithm to the sampling rate, its sidelobe suppression performance is weaker in the azimuth direction. During the SAR image acquisition process, the sampling rate variation in the range direction is relatively small, leading to better sidelobe suppression performance. Therefore, by applying the SVA algorithm for sidelobe suppression to SAR data in the range direction of different images, and inputting the resulting data into a deep learning network, the network can learn the suppression characteristics under different sampling rates. By learning these features,

the neural network can effectively suppress sidelobes even when the sampling rate changes. In other words, it can effectively remove sidelobes in the azimuth direction.

The design of the SVA-Net network is based on the SVA algorithm. The SVA algorithm can be simplified as shown in Figure 2:

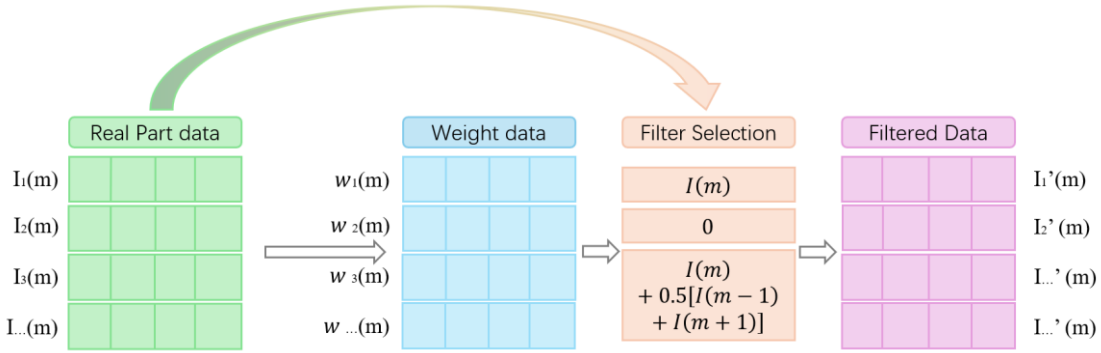

Figure 2.Flowchart of the SVA Algorithm.

The SVA algorithm processes the real and imaginary parts of the SAR complex data separately. During the process, the real and imaginary parts of the data are subjected to sidelobe suppression along the rows and columns, respectively. As shown in the figure above, $\mathrm{I_i(m)}$ represents the real part of the SAR image data in the row direction. By traversing this row, the weight values $\mathrm{w_i(m)}$ at different points are obtained. Then, based on these weight values, different filters are applied to process the point values, resulting in the filtered data. Therefore, when designing the deep learning network, this process is referenced to design the weight generation module and the filter generation module. The weights and filter outputs are then multiplied to obtain the final sidelobe suppression result for the SAR image.

In SVA-Net, the design of the weight generation module is inspired by the process of generating weight data. This module utilizes Convolutional Neural Networks (CNN) to process array elements and generate weights. Specifically, the convolutional layers extract local features from the input data, and the neural network learns how to map these features to the target weight values.

As shown in Figure 3, in the weight generation module, the input tensor of shape 1x256 first passes through a convolutional layer, where both the kernel size and the number of kernels are set to 15, with appropriate padding. Then, after normalization and activation functions, the output is a tensor of shape 15x256, representing 15 sets of weights that will be used in subsequent steps. In typical CNNs, the kernel size is usually set to 3, but in this network, to enhance the model's ability to perceive data, the kernel size is set to 15, which expands the receptive field and allows the model to better capture broader contextual information.

The filter generation module of SVA-Net cleverly adopts the multi-layer pyramid structure of U-Net and combines it with both shallow and deep features to achieve efficient signal processing. The design of this structure effectively integrates features from different layers, allowing for the simultaneous processing of both local and global information in the signal, and thereby generating filters suitable for various signal processing tasks. Specifically, shallow features, with their smaller receptive fields, can capture detailed information in the signal, particularly in the high-frequency components, where they can accurately identify and distinguish subtle variations in the signal, such as fluctuations in the mainlobe and sidelobes. This is crucial for the fine processing of high-frequency signals. On the other hand, deep features, with their larger receptive fields, can analyze the global characteristics of the signal, especially in the low-frequency components, where they model the complex pulse responses, helping to understand the superposition effects of different pulse responses and various coupling effects in the signal. The combination of shallow and deep features enables SVA-Net to focus on details while capturing global information, demonstrating powerful capabilities and efficiency in signal filtering and feature extraction.

In SVA-Net, to restore the mainlobe energy and effectively suppress the sidelobes, a Generative Adversarial Network (GAN) design is adopted. In this network, the generator generates the denoised signal by multiplying the dynamically learned weights with the filter, while the discriminator is used to distinguish the differences between the generated signal and the real signal. During the training process, the loss function penalizes the mainlobe regions, forcing the generator to

produce signals that are as close to the real data as possible in these regions. This approach successfully restores the mainlobe energy. By introducing the weighted loss function, the discriminator will focus more on the mainlobe region of the signal during training, thereby helping the generator recover a more accurate mainlobe signal.

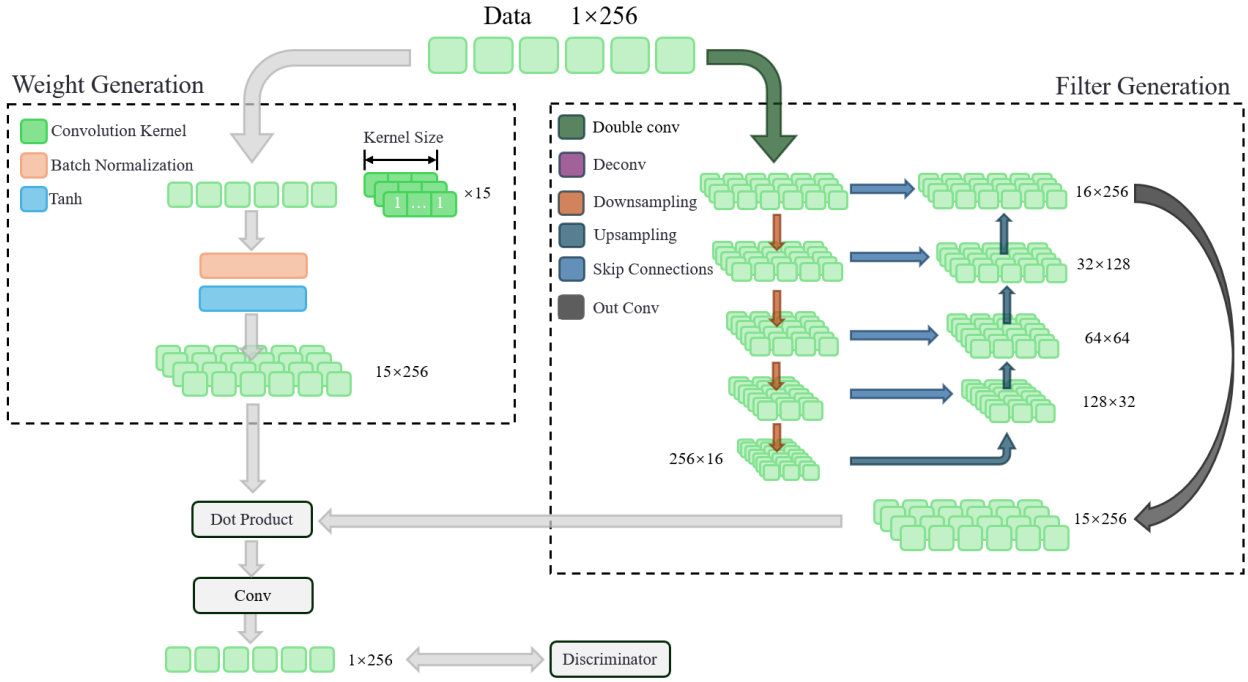

Figure 3. SVA-Net Network Architecture.

3. Experiments Results and Analysis

3.1 Dataset

The purpose of this experiment is to use neural networks to learn the sidelobe suppression characteristics of the SVA algorithm in the range direction and extend it to sidelobe suppression in the azimuth direction. For this purpose, 11 large-scene SAR complex data images were selected as the research objects. Since these images have inconsistent resolution in the range and azimuth directions, directly applying the spatial variance algorithm for unified processing is challenging. Therefore, each of the 11 images was processed separately to form 11 independent data sets.

For each data set, regions with significant sidelobe interference were first identified, and these regions were cropped into 256x256 pixel blocks. Then, data containing the sidelobes and their adjacent columns were extracted from each region to form 1x256 vectors. In total, 680 sidelobe column data were extracted from the 11 SAR images using the above method.

The column data were grouped according to different criteria, and the SVA algorithm was applied to batch process the sidelobe column data with corresponding parameters for sidelobe suppression, resulting in pairs of sidelobe and suppressed sidelobe column data. Since these data come from different SAR images, normalization was applied. This resulted in a dataset of 680 paired data entries. The data were then split into training, testing, and validation sets in an 8:1:1 ratio for training and evaluating the neural network model. A visualization of part of the training set is shown in Figure 4.

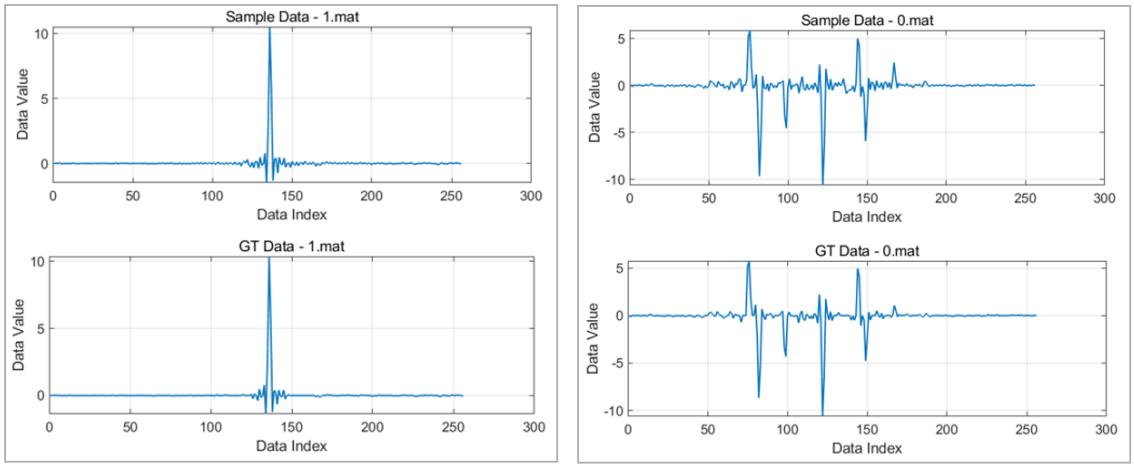

(a) (b)

Figure 4. Figures (a) and (b) show two sets of data before and after sidelobe suppression. The top part displays the original data without suppression, while the bottom part shows the data after suppression has been applied.

3.2 Experimental Results and Analysis

To verify the sidelobe suppression effect learned by the SVA-Net network, a complex SAR slice of size 256x256 was processed. As shown in Figure 5(a), the corner reflector produces strong cross-shaped sidelobe interference due to strong reflection. The data was divided by rows and columns and input into the SVA-Net network, resulting in the images shown in Figure 5(b) and Figure 5(c). It can be observed that the sidelobe interference was accurately removed, but noise appears in the background where there are no targets; this noise is caused by the low scattering values in the background region which, after being normalized by the network, inadvertently amplified the background clutter.

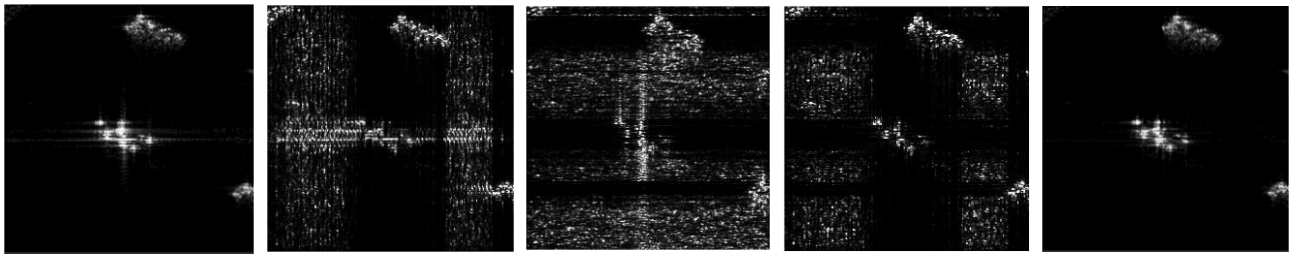

(a) (b) (c) (d) (e)

Figure 5. Visualization of the Sidelobe Suppression Process.

A simple method to remove background noise while retaining the sidelobe suppression effect involves taking the mathematical intersection between Figure 5(b) and Figure 5(c) to obtain an image that retains the sidelobe suppression effect. By comparing this intersected image with the input image and selecting the minimum values, the final image Figure 5(e) can be generated, thereby removing the background noise while preserving the sidelobe suppression effect.

In summary, Figure 5(a) displays the initial dataset before sidelobe suppression, Figure 5(b) shows the result of column-wise suppression reducing sidelobes along the columns, Figure 5(c) illustrates the row-wise suppression minimizing sidelobes along the rows, Figure 5(d) presents the intersection of (b) and (c) obtaining the target image with effectively suppressed sidelobes, and Figure 5(e) displays the result of calculating the minimum ratio between the processed data in (d) and the original data in (a), ensuring the most conservative suppression for the final sidelobe-suppressed image.

To further validate the applicability of the method, a comparison was made between the results of the SAV algorithm and those of SAV-Net. The data processed were sourced from MiniSAR data collected by our laboratory's drones and TerraSAR-X satellite data. Since the baseline processing size for SVA-Net is 256x256, sidelobe suppression for larger SAR images is achieved by dividing the input image into segments of 256x256 pixels before inputting them into the

network for processing; if the segment is smaller than 256x256, it is padded with zeros to reach the required size, and then the processing is carried out.

The experimental results are shown in Figures 6, 7, and 8.

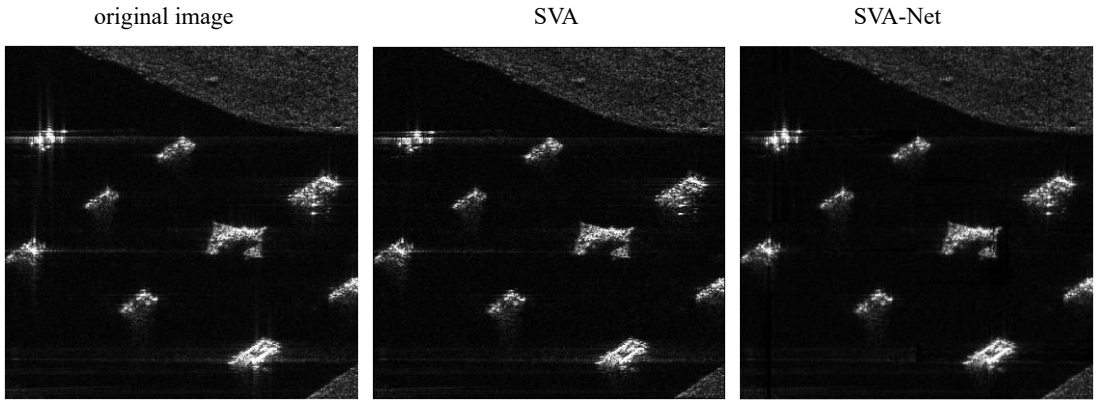

Figure 6. Processing results of vehicle sidelobes using the SVA algorithm and the algorithm proposed in this paper. The data source is the MiniSAR data collected in this experiment.

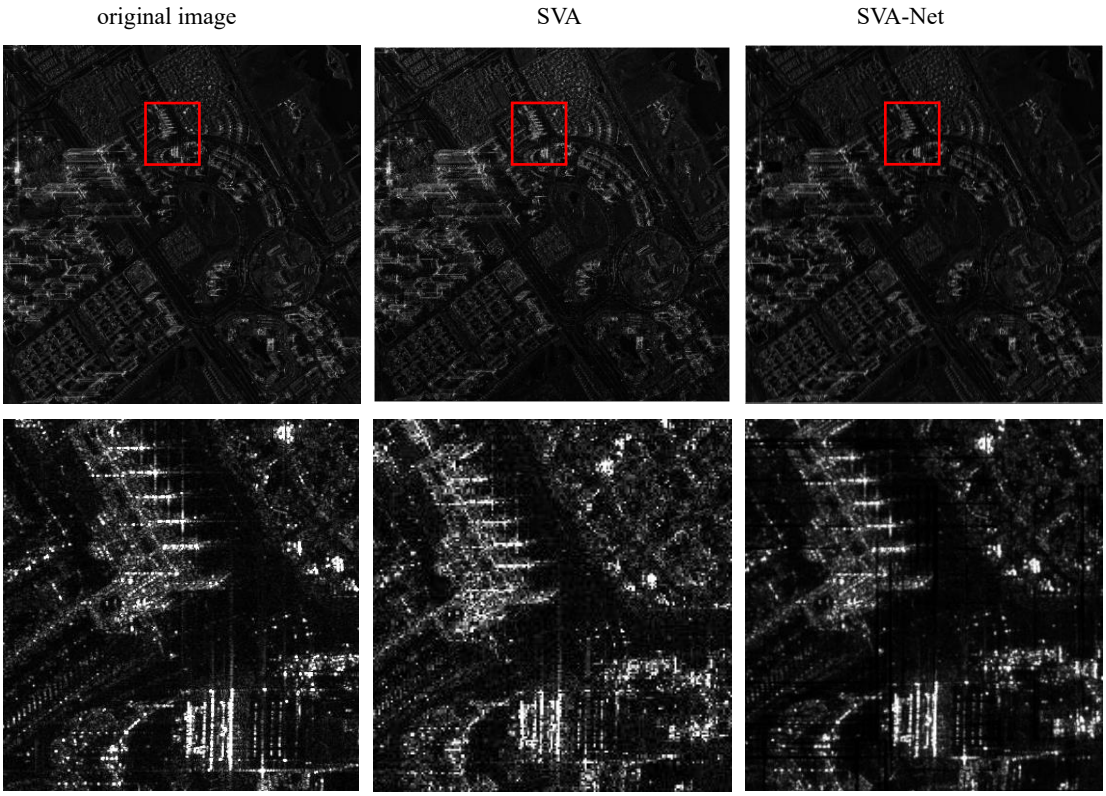

Figure 7. Processing results of sidelobes in urban areas. The first row shows panoramic images, and the second row provides enlarged views of the areas within the red boxes. The images are sourced from TerraSAR-X data of Dubai's urban area.

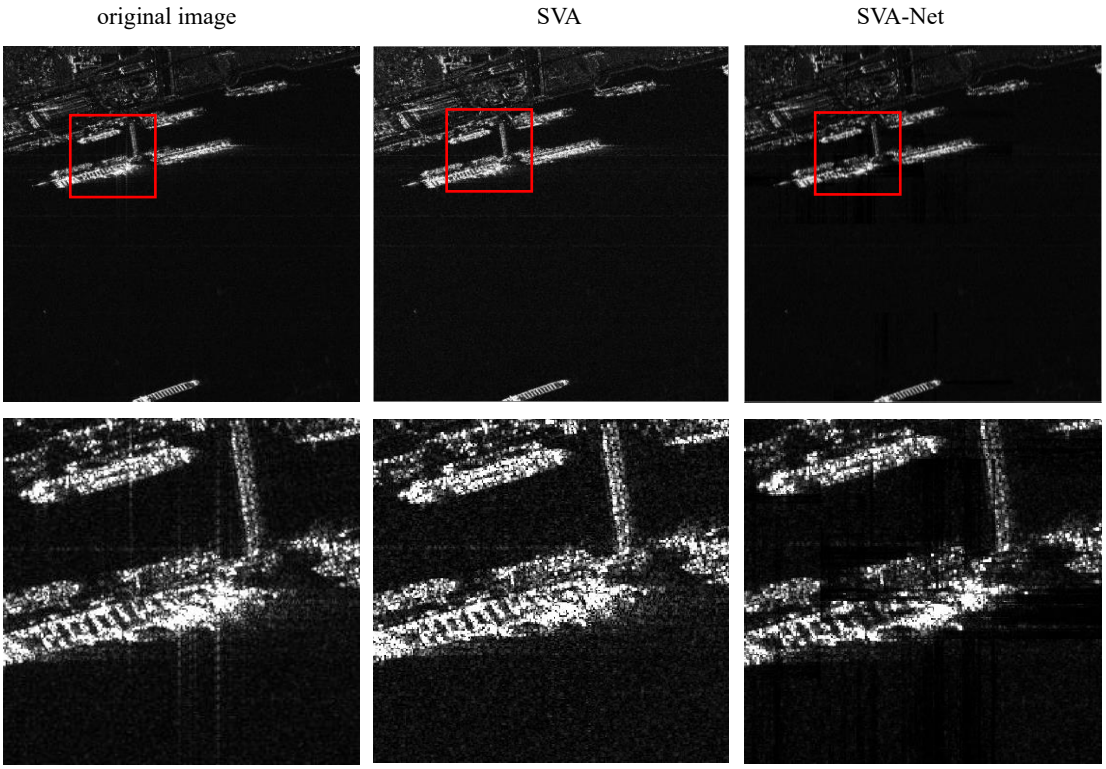

Figure 8. Processing results of ship sidelobes. The first row shows panoramic images, and the second row provides enlarged views of the areas within the red boxes. The images are sourced from TerraSAR-X data of the port of Shanghai.

From the aforementioned comparative results, it can be seen that the SVA algorithm performs well in range sidelobe suppression but has poor performance in azimuth sidelobe suppression, with horizontal direction sidelobes still present. In contrast, the images processed by SVA-Net effectively remove both vertical and horizontal sidelobes. This demonstrates that SVA-Net successfully learned the range sidelobe suppression characteristics of the SAV algorithm and applied them effectively to azimuth sidelobe suppression.

However, the suppression effect on large scenes is not as good as that on small scenes. The reason for this is analyzed as follows: the foundation of SAV-Net is based on processing SAR images of size 256x256, which imposes limitations when handling large scene images. When segmenting large scene images into 256x256 regions, it cannot guarantee that sidelobes and targets will simultaneously appear within the same region. When sidelobes appear alone, they may be identified as background and thus not processed.

3.3 Analyses of Processing Efficiency

This section analyzes the time efficiency of SVA-Net and provides its processing frame rates on different hardware devices. Since time efficiency can be influenced by factors such as implementation details and hardware, the computational complexity is also measured in terms of floating-point operations (FLOPs) for a more objective analysis.

According to the FLOP results, most of the computational load comes from the convolution operations in the filter generation module. Due to the explicit analytical solution of the SVA algorithm, its computational complexity is much lower than that of SVA-Net. The FLOPs calculation for SVA-Net is shown in Figure 9.

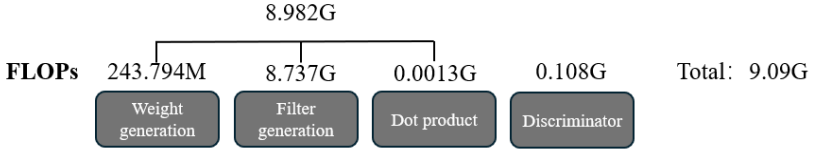

Figure 9. Schematic diagram of FLOPs calculation for SVA-Net

Using a 512x512 complex SAR image as an example, Table 1 lists the processing frame rates of SVA-Net on different hardware, tested on a CPU (Intel i5-13400) and a GPU (GeForce GTX 1060). It can be seen that SVA-Net is slightly faster than the SVA algorithm. This is primarily because SVA-Net leverages batch processing for parallel computation when handling rows or columns, whereas the SVA algorithm performs serial computation, resulting in a slight speed advantage for SVA-Net.

Table 1. Information on video and audio files that can accompany a manuscript submission.

Device	CPU	GTX 1060
SVA Frame Rates	2.22fps	-
SVA-Net Frame Rates	3.23fps	9.79fps

4. Conclusion

This paper builds upon the traditional SVA algorithm, pointing out its limitations, such as the strict sampling rate requirements, good sidelobe suppression in the range direction but poor suppression in the azimuth direction. To address these issues, the paper proposes the construction of the SVA-Net network. By referencing the processing flow of the SVA algorithm, SVA-Net integrates a weight generation module and a filter generation module. Using the SVA algorithm, a dataset was created with data that shows good sidelobe suppression in the range direction, paired with the original data, for SVA-Net to learn the characteristics of sidelobe suppression. Additionally, a discriminator was incorporated to restore mainlobe energy.

The analysis of results from real data demonstrates that the learned SVA-Net not only overcomes the sampling rate requirements of the original data but also significantly improves sidelobe suppression in the azimuth direction compared to the traditional SVA algorithm. Furthermore, the mainlobe energy has been well restored.

However, due to limitations in training data size and network input dimensions, the adaptability of SVA-Net to larger image sizes still has room for improvement. Future research could further explore longer processing networks or region-specific suppression methods, and try optimizing the network structure by extending the one-dimensional network to a two-dimensional network to enhance processing speed and efficiency. Additionally, exploring multi-scale feature extraction and adaptive filtering strategies could further enhance sidelobe suppression capabilities.

REFERENCES

[1] Rodriguez, E. and Martin, J. M., "Theory and design of interferometric synthetic aperture radars", IEE Proc. F Radar Signal Process., vol. 139, no. 2, pp. 147-159, Apr. 1992.

[2] Curlander, J. C. and McDonough, R. N., Synthetic Aperture Radar, vol. 11, 1991.

[3] Yang, H. and Wang, J., “Sidelobe suppression of sar images by spectrum shaping,” in IGARSS 2022-2022 IEEE International Geoscience and Remote Sensing Symposium, 2022, pp. 1668–1671.

[4] Stankwitz, H., Dallaire, R., and Fienup, J., “Nonlinear apodization for sidelobe control in sar imagery,” IEEE Transactions on Aerospace and Electronic Systems, vol. 31, no. 1, pp. 267–279, 1995.

[5] Castillo-Rubio, C., Llorente-Romano, S., and Burgos-Garcia, M., “Robust sva method for every sampling rate condition,” IEEE Transactions on Aerospace and Electronic Systems, vol. 43, no. 2, pp. 571–580, 2007.

[6] Yuan, L., Haoyue, S., Yong, H., et al., “Low sidelobe NLFM waveform design based on phase function construction method,” Fire Control Radar Technology, 2024, 53(03): 1-9. DOI: 10.19472/j.cnki.1008-8652.2024.03.001.

[7] Xiang, D., Li, W., Sun, X., Wang, H., and Su, Y., "Sidelobe Suppression for High-Resolution SAR Imagery Based on Spectral Reshaping and Feature Statistical Difference," in IEEE Transactions on Geoscience and Remote Sensing, vol. 62, pp. 1-14, 2024, Art no. 5211314, doi: 10.1109/TGRS.2024.3394405.